# Valence states of Yb in $Yb_5Si_3$

M. Rams and K. Królas
*Institute of Physics, Jagiellonian University, 30-059 Kraków, Poland*

P. Bonville
*CEA, Centre d'Etudes de Saclay, Département de Recherche sur l'Etat Condensé, les Atomes et les Molécules, 91191 Gif-sur-Yvette, France*

E. Alleno and C. Godart
*CNRS, Place Aristide Briant, 92000 Meudon, France*

D. Kaczorowski
*W. Trzebiatowski Intitute for Low Temperature and Structure Research, Polish Academy of Science, 50-950 Wroclaw, Poland*

F. Canepa
*Dipartimento di Chimica e Chimica Industriale, 16146 Genova, Italy*
(Received 18 March 1997)

We have measured the quadrupole hyperfine interaction in the intermetallic compound $Yb_5Si_3$ using $^{170}Yb$ Mössbauer absorption spectroscopy in the temperature range 0.03–80 K and $^{172}Yb$ perturbed angular correlation spectroscopy in the temperature range 20–750 K. Data of $L_{III}$-edge x-ray absorption and magnetic susceptibility are also presented, as well as a $^{170}Yb$ Mössbauer spectrum with a magnetic field of 7 T at 4.2 K. There are two distinct crystallographic sites for Yb in $Yb_5Si_3$. The whole set of our measurements shows that the two sites contain Yb ions in a charge state close to 3+, but with different hybridization strengths, making $Yb_5Si_3$ a unique compound. No magnetic ordering of the $Yb^{3+}$ sublattice is shown down to a temperature of 0.03 K. [S0163-1829(97)07231-7]

## I. INTRODUCTION

The ytterbium silicide family consists of several compounds with different magnetic properties and charge states for the Yb ion.[1] The alloy $Yb_3Si_5$ contains Yb ions in a mixed-valence state close to the divalent state.[2] In YbSi, the Yb ions appear as almost trivalent, and show Kondo properties.[3] This compound orders magnetically below $T_N = 1.6$ K with a very small $Yb^{3+}$ spontaneous moment.[4] The first measurements performed on the metallic alloy $Yb_5Si_3$ (Ref. 5) seemed to imply that, contrary to both above-mentioned silicides, it is not a homogeneous but a heterogeneous mixed-valence system which has its two crystallographically inequivalent Yb sites occupied by divalent and trivalent ions.

The valence states of Yb in solids can be studied in several ways. Trivalent Yb has a $4f^{13}$ configuration with $J=\frac{7}{2}$ and is paramagnetic, while $Yb^{2+}$, with a $4f^{14}$ ground state and $J=0$, is diamagnetic. Therefore a conclusion on the Yb valence states can be drawn from the magnetic properties of the crystal. One is also able to distinguish between the two types of ions using photoemission or $L_{III}$-edge x-ray-absorption techniques since they both are sensitive to the electron binding energy which is characteristic for a given charge state. Finally, there are some hyperfine interaction methods like Mössbauer spectroscopy or the perturbed angular correlation (PAC) of $\gamma$ radiation where the valence state can be inferred from the measurement of the electric quadrupole interaction and of its thermal behavior.

In noncubic compounds, the quadrupole moment of the nuclei is submitted to an electric-field gradient (EFG). This EFG originates from all extranuclear charges. For the Yb ion, the essential point is that for divalent and trivalent ions, there are quite different contributions to the EFG from the self-ion electronic shell. The $Yb^{2+}$ ions have a completely filled $4f$ electron shell, and in such a case the $4f$ electrons do not contribute directly to the EFG at a nucleus, which then arises only due to the surrounding atomic charges in the crystal lattice. For $Yb^{3+}$ ions, there is large contribution to the EFG from the partially filled $4f$ electron shell, arising from the $4f$ level splitting in the crystal electric field (CEF). The CEF sublevels contribute to the EFG in different amounts, and their population changes with increasing temperature according to the Boltzmann distribution. Therefore, while the lattice contribution to the EFG is practically temperature independent, the contribution from the unfilled $4f$ shell shows a strong temperature variation. At low temperature the $4f$ contribution is usually dominant, but it vanishes at very high temperature when the CEF sublevels are equally populated.

Here we present a study of the Yb valence in the intermetallic compound $Yb_5Si_3$ using the following microscopic techniques: Mössbauer absorption spectroscopy with the isotope $^{170}Yb$, $\gamma$-$\gamma$ perturbed angular correlations in $^{172}Yb$, and x-ray absorption at the Yb $L_{III}$ edge. Additionally, the existing magnetic-susceptibility measurements were extended to higher temperature (up to 800 K). $Yb_5Si_3$ was previously supposed to be an example of a compound with $Yb^{3+}$ and

 

$Yb^{2+}$ ions occupying the two inequivalent lattice sites. This was concluded from the susceptibility measurements up to room temperature,[5] and from photoemission measurements.[1] The results of our hyperfine interaction experiments, the $L_{III}$-edge spectroscopy, as well as the high-temperature magnetic-susceptibility measurements contradict such a picture, making $Yb_5Si_3$ a more stimulating compound than expected. A preliminary account of this work was published in Ref. 6.

## II. EXPERIMENT

### A. Crystal structure

The preparation of the sample is described in Ref. 5. In all the experiments polycrystalline powder samples were used. $Yb_5Si_3$ crystallizes into a $Mn_5Si_3$-type hexagonal structure (space group $P6_3/mcm$). In this structure, the rare-earth atoms occupy two crystallographically inequivalent sites which correspond to the Wyckoff positions $4d$ and $6g$. The 40% of Yb ions at the $4d$ site have an axial symmetry ($D_{3h}$ point group), while the rest ($6g$ site) lies at a site with less than threefold symmetry ($C_{2v}$ point group). An x-ray diffractogram of the sample shows the lines of the $Mn_5Si_3$-type structure with $a=8.251$ Å and $c=6.231$ Å. Weak intensity lines pertaining to impurity phases are observed, amounting to no more than a few percent of the sample mass: one or two lines of Si and of Yb could be identified, and other lines remain of undetermined origin. We emphasize that no lines pertaining to other Yb silicides ($Yb_3Si_5$ or YbSi) are present.

### B. Mössbauer effect measurements

The Mössbauer transition for the $^{170}$Yb isotope has an energy 84.3 keV, and links the ground state ($I_g=0$) and the first excited state ($I=2$). The Doppler velocity-energy conversion factor is 1 mm/s = 68 MHz for $^{170}$Yb. A monochromatic $\gamma$-ray source of $^{170}$Tm* in $TmB_{12}$ was used to record the spectra; the full width at half maximum of the source line is 3 mm/s with respect to a $YbAl_3$ reference absorber. Measurements were carried out in the temperature range from 30 mK to 80 K. Spectra below 1.4 K were recorded using a $^3$He-$^4$He dilution refrigerator. A spectrum was also recorded at 4.2 K with a magnetic field of 7 T applied perpendicularly to the $\gamma$-ray propagation direction.

### C. Perturbed angular correlation measurements

Contrary to Mössbauer spectroscopy, which, due to the temperature-dependent recoilless factor, allows the hyperfine interaction of $^{170}$Yb to be measured only up to about 100 K, the PAC measurement sensitivity is practically temperature independent. The PAC spectra were recorded at several temperatures in the range from 20 to 750 K. We used the 91–1094-keV $\gamma$-$\gamma$ cascade emitted after the radioactive decay of $^{172}$Lu to the excited states of $^{172}$Yb. The intermediate level of the cascade is characterized by the nuclear spin $I=3$ and the half-life $T_{1/2}=8.3$ ns. The radioactive samples were obtained by deuteron irradiation of the $Yb_5Si_3$ compound itself. The $^{172}$Lu isotope was produced in the target as a result of the $^{172}$Yb$(d,2n)^{172}$Lu nuclear reaction. After the irradiation, the sample was sealed in a quartz tube and then placed into a small oven or cryostat in a PAC setup. The PAC measurements were carried out using a conventional slow-fast coincidence system equipped with four $BaF_2$ detectors. Since the $^{172}$Lu activity decays with a half-life of 6.7 days, one sample can be used for 3–4 weeks until the activity drops below a suitable level.

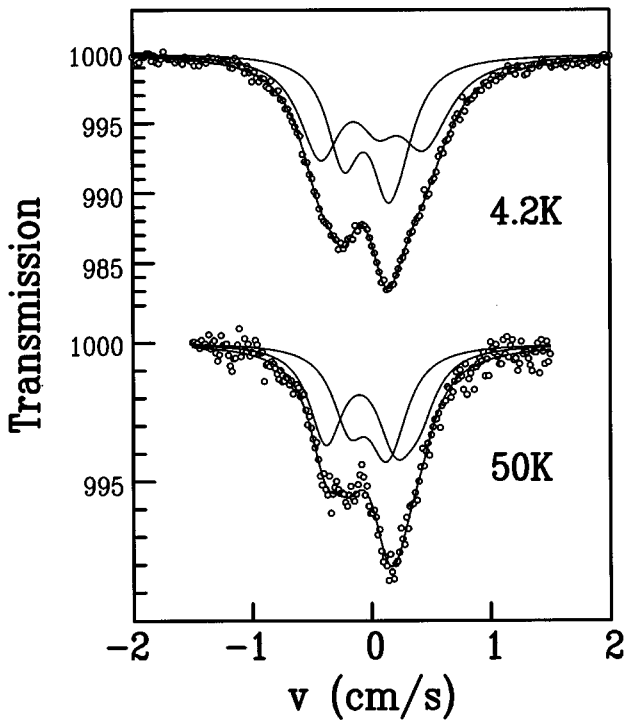


FIG. 1. $^{170}$Yb Mössbauer absorption spectra in $Yb_5Si_3$ in zero field at $T=4.2$ and 50 K. The spectral decomposition performed in the fits are marked with solid lines.

### D. Magnetic and x-ray-absorption measurements

The magnetic susceptibility $\chi$ was measured with a superconducting quantum interference device with a field of 0.5 T in the temperature range 1.7–800 K. The x-ray-absorption measurements [x-ray-appearance near-edge structure (XANES)] were performed at the French Synchrotron Radiation Facility (LURE) in Orsay, at two temperatures 10 and 300 K, in the photon energy range 8940–9020 eV which contains the $L_{III}$ edge of Yb. Experimental details concerning the XANES technique can be found in Ref. 7.

## III. ANALYSIS OF THE HYPERFINE DATA IN ZERO FIELD

The shape of the zero-field Mössbauer spectra (Fig. 1), as well as the perturbation patterns of the PAC spectra (Fig. 2), contain all the relevant information on the hyperfine interaction. In the whole temperature range, the spectra show that a hyperfine electric quadrupole interaction alone is present. The $^{170}$Yb Mössbauer measurements down to 0.03 K could not detect any magnetic interaction nor any significant broadening of the lines, which means that neither of the Yb sublattices show any magnetic ordering down to 0.03 K.

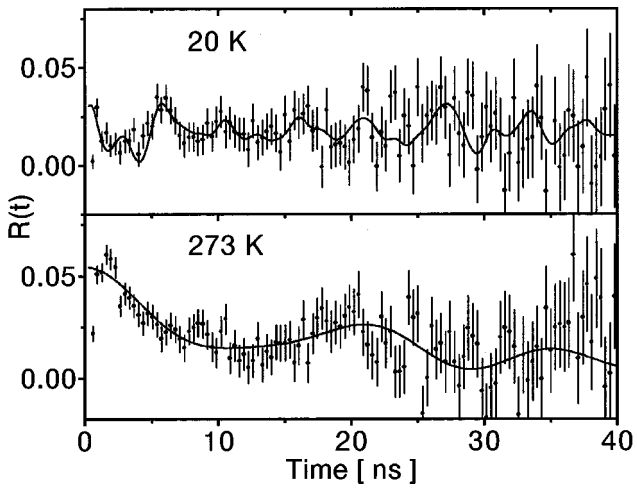


FIG. 2. Perturbed angular correlation spectra of $^{172}$Yb in $Yb_5Si_3$ at 20 and 273 K. The solid lines represent fits of the perturbation factor to a superposition of two static quadrupole interaction components.

The hyperfine electric quadrupole Hamiltonian is conventionally written as

$$H_Q=\frac{eQV_{zz}}{4I(2I-1)}\left[3I_z^2-I(I+1)+\eta\frac{(I_-^2+I_+^2)}{2}\right], \qquad (1)$$

where the diagonalized EFG tensor $\{V_{xx},V_{yy},V_{zz}\}$ is represented by two independent parameters: its largest component $V_{zz}$ and the asymmetry parameter $\eta=(V_{xx}-V_{yy})/V_{zz}$. The interacting nucleus is described by its electric quadrupole moment $eQ$ and its spin $I$. To compare results from the Mössbauer and PAC measurements, the different spins and various quadrupole moments $Q$ of the involved isotopes should be taken into account. We adopt $Q^{170}=-2.14$ b (Ref. 8) as the quadrupole moment of $^{170}$Yb in the 84-keV excited state with spin $I=2$ and $Q^{172}=3.1$ b (Ref. 9) for $^{172}$Yb in the 1172-keV excited state with spin $I=3$. It should be noticed here that only the absolute value of $V_{zz}$ can be derived from a $\gamma$-$\gamma$ PAC measurement while the sign of $V_{zz}$ can be determined from the $^{170}$Yb Mössbauer spectra. It was found that both the Mössbauer and PAC spectra consist of two components. These components are identified with the two inequivalent Yb sites in the crystal lattice of $Yb_5Si_3$.

In the PAC spectra, the relative amplitudes of both components practically do not vary with temperature. The major component is equal to about 60% [from 54(3)% to 64(4)% for different spectra]. It agrees very well with the site occupation ratio 3:2 for the two $6g$ and $4d$ Yb sites in $Yb_5Si_3$. For the minor component the EFG tensor appears to be axial ($\eta=0$ in the limit of the experimental error). This result agrees with the expectation coming from the crystal lattice symmetry: the EFG tensor is axial at a lattice site with a threefold or higher symmetry axis like the $4d$ site. In the final step of the fitting procedure, the two amplitudes were fixed to be 60% and 40%, and $\eta$ was kept equal to zero for the 40% component. The fitted parameters were then the two quadrupole interaction frequencies $\nu_Q=eQ^{172}|V_{zz}|/h$ and the asymmetry parameter $\eta$ for the 60% component. The $|V_{zz}|$ values derived from the $\nu_Q$ values, as well as $\eta$, are plotted in Fig. 3 with circles. The asymmetry parameter can

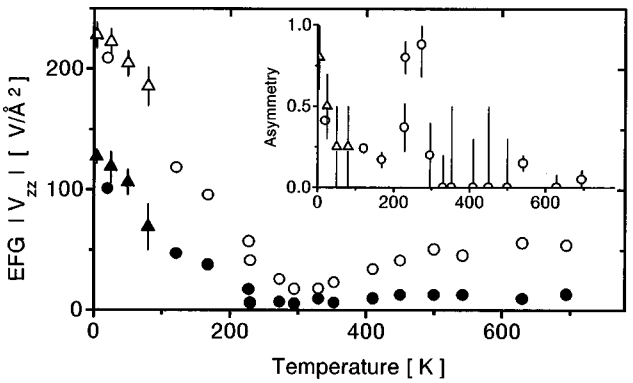


FIG. 3. Temperature dependence of the quadrupole interaction parameters $\eta$ and $|V_{zz}|$ for the two Yb sites in $Yb_5Si_3$. The Mössbauer effect data are denoted with triangles, and the PAC data with circles. Data for the $4d$ site are marked with open symbols, and for the $6g$ site with solid symbols.

be determined with a rather good accuracy when the frequency $\nu_Q$ is high enough. When the quadrupole interaction becomes very weak (in the range 200–400 K), the fitted value of $\eta$ is no longer reliable.

In the zero-field Mössbauer spectra, the two components are not resolved, but fits allowing for only a single quadrupolar interaction are not satisfactory. Using two quadrupolar components, we find an amplitude ratio again near to 3:2. The best-resolved spectrum at 4.2 K gives the ratio 57(3):43(3). Besides the intensity of the two components, the fitted parameters were the quadrupole coupling constants $\alpha_Q=eQ^{170}V_{zz}/8$ for both components and the asymmetry parameter $\eta$ for the 60% component. At 4.2 K, the fitted values are $\alpha_Q=-2.15(10)$ mm/s and $\eta=0.8(0.2)$ for the 60% component, and $\alpha_Q=-1.20(10)$ mm/s for the 40% component. In principle, the Mössbauer effect measurements can yield additional information concerning the valence state, i.e., the isomer shift value. However, for $^{170}$Yb the experimental linewidth (3 mm/s) is much larger than the difference in the isomer shifts for $Yb^{3+}$ (0.1–0.2 mm/s) and $Yb^{2+}$ ($-0.3$–$-0.1$ mm/s) ions.[10] Therefore, a reliable value for the isomer shift can only be obtained from good statistics spectra with simple and well-resolved line shapes. The spectrum taken at 4.2 K, which has the best statistics, yields isomer shifts values of 0.25 and 0.15 mm/s (relative to the $TmB_{12}$ source) for the 60 and 40% component, respectively. These values are in the range for trivalent Yb ions in a metallic host,[10] but they are not too reliable because of the poor resolution of the spectrum.

The fitted EFG parameters for two Yb sites are shown together in Fig. 3 for the Mössbauer and PAC data. We plotted the quantity $|V_{zz}|$ as determined by PAC measurements, but the Mössbauer-derived $\alpha_Q$ is negative for both sites, which means that $V_{zz}$ is positive (at least below 80 K). The results obtained with the two techniques are in satisfactory agreement. The important result is that the principal component of the EFG tensor drops by a factor of 5 between 4 and 200 K for both sites. In the same temperature range the $\eta$ value of the 60% component decreases from 0.8 to about 0.2. It seems that three components of the EFG tensor decrease with temperature at different rates, and a sudden jump of the $\eta$ parameter above 200 K corresponds to a change of the

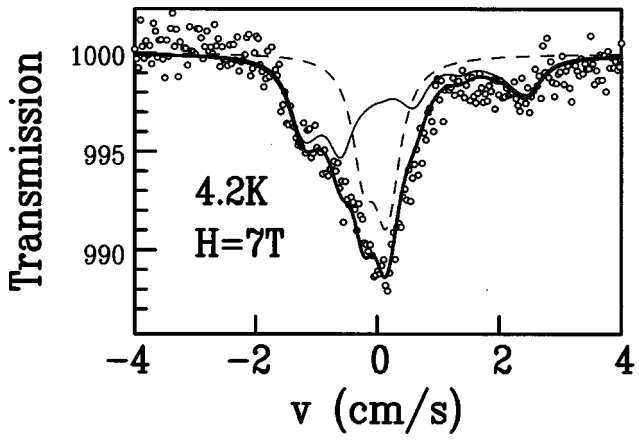


FIG. 4. $^{170}$Yb Mössbauer absorption spectrum in $Yb_5Si_3$ at 4.2 K with a magnetic field of 7 T applied perpendicularly to the $\gamma$-ray propagation direction.

principal EFG axes. The observed strong temperature dependence of the EFG tensor clearly indicates that, at both sites, the $4f$ electrons contribute to the EFG at the Yb nucleus, i.e., that both Yb ions are trivalent or close to trivalent.

## IV. IN-FIELD $^{170}$YB MÖSSBAUER SPECTRUM AT 4.2 K

The Mössbauer spectrum at 4.2 K with an applied field of 7 T, shown in Fig. 4, is quite different from the zero-field spectrum shown in Fig. 1. It can be analyzed with two components. The central absorption corresponds to a quadrupolar hyperfine interaction (the dashed line in Fig. 4), with $\alpha_Q \simeq -1.2$ mm/s and a weight of approximately 40%, and the split absorption to a magnetic hyperfine interaction. In the first step, fitting this latter component into the hyperfine field approximation, one obtains a satisfactory fit with a hyperfine field of 225 T (corresponding to a $Yb^{3+}$ magnetic moment of $\simeq 2.2\mu_B$, using the $^{170}Yb^{3+}$ hyperfine proportionality constant $C = 102$ T/$\mu_B$) and an axial quadrupolar interaction with $\alpha_Q \simeq 3$ mm/s. These two components are identified with the Yb ions in the two crystallographic sites. These data show that the local magnetic susceptibility is quite different for the two Yb ions in the two sites. For the 40% component (the $4d$ site), the Mössbauer spectrum is unchanged (within experimental error) in the presence of the magnetic field of 7 T, i.e., the magnetic susceptibility of the corresponding Yb ions is very small at 4.2 K, like for a $Yb^{2+}$ ion. The Yb ions in the 60% component ($6g$ site), by contrast, show a large paramagnetic susceptibility, with a ratio $m(H=7T)/H \simeq 0.18$ emu/mole at 4.2 K.

In the paramagnetic phase at low temperature, the powder Mössbauer measured in a magnetic field is not a simple hyperfine field spectrum in the case of the ground CEF doublet of a $Yb^{3+}$ ion in a site with symmetry lower than cubic. Indeed, the CEF anisotropy implies that the direction and size of the paramagnetic moment induced by the applied field depends on the orientation of the local crystal axes with respect to the field. The Mössbauer spectrum should then be calculated as a powder average, and it depends on the electronic $g$ tensor and the EFG tensor of the ground $Yb^{3+}$ state. Such a procedure should be applied for Yb ions at the $6g$ site in $Yb_5Si_3$, which occupy a site with low symmetry. However, for such a site, with a symmetry lower than axial, the number of parameters (the principal values of the tensors and the angles defining their relative orientation) is large. We used the approximation of axial symmetry to fit the 60% component in the in-field spectrum of $Yb_5Si_3$. The thin solid line in Fig. 4 represents the result of such a fit, which is markedly better than the hyperfine field fit done as a first approximation. The obtained parameters are characteristic of a rather anisotropic CEF doublet: $g_z \simeq 5$ and $g_\perp / g_z \sim 0.1$, and $\alpha_Q \simeq 3$ mm/s. This quadrupolar coupling parameter is of an opposite sign to the zero-field value ($-2.1$ mm/s); this can be due to the mixing effect of the 7-T field which can be expected to modify the wave functions of the CEF states, or it can be an artifact due to the axial approximation used in the calculation of the line shapes.

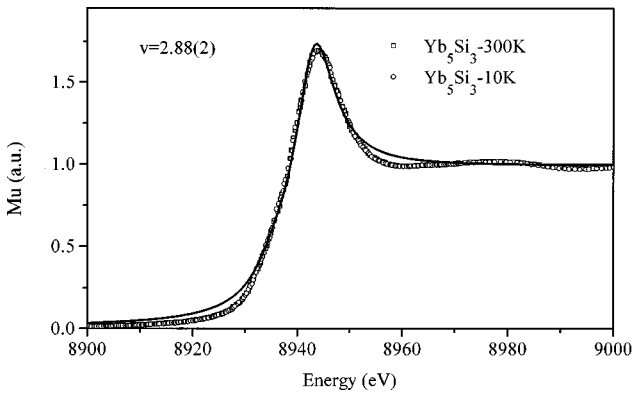


FIG. 5. X-ray-absorption spectra near the Yb $L_{III}$ edge for $Yb_5Si_3$ at 10 and 300 K.

## V. X-RAY ABSORPTION AT THE YB $L_{III}$ EDGE (XANES)

The zero-field hyperfine measurements suggesting the presence of trivalent (or close to trivalent) Yb on both sites in $Yb_5Si_3$, and the Mössbauer spectrum with 7 T showing that only the 60% Yb component has a magnetic susceptibility characteristic of $Yb^{3+}$, we performed x-ray-absorption spectra at the Yb $L_{III}$ edge in order to obtain an independent determination of the Yb valence. The spectra at both temperatures (10 and 300 K) are practically identical (see Fig. 5). The dominant peak at an energy $\sim 8943$ eV is associated with the $Yb^{3+}$ valence state. At $\sim 8935$ eV there is another weak component which indicates the presence of the $Yb^{2+}$ valence state. The spectra were fitted in the standard way,[7] allowing for Lorentzian-shaped peaks and arc-tangent functions for the background. The derived relative weight of the two peaks gives a mean Yb valence equal to $v = 2.88(2)$ at both temperatures. This is much larger than the value of 2.6 expected with the hypothesis of three $Yb^{3+}$ and two $Yb^{2+}$ ions in the unit cell. If one assumes that the $6g$ Yb ions are purely trivalent, then the experimentally obtained valence $v = 2.88$ implies that the lower limit for the valence of the $4d$ Yb ions is 2.7.

## VI. MAGNETIC SUSCEPTIBILITY

The inverse molar magnetic susceptibility of $Yb_5Si_3$ in the temperature range 1.7–800 K is shown in Fig. 6. Above 100 K the $\chi^{-1}(T)$ dependence follows a modified Curie-

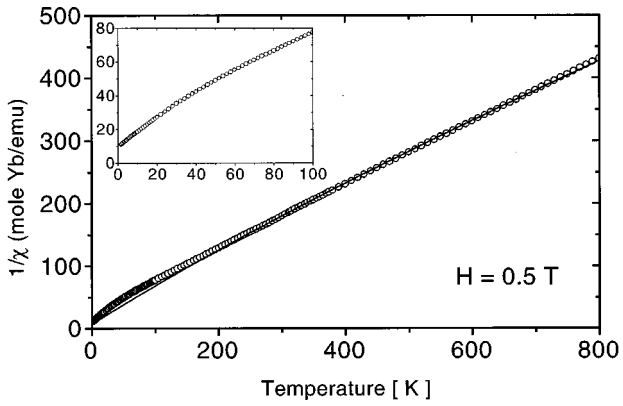


FIG. 6. Inverse of the magnetic susceptibility vs temperature for $Yb_5Si_3$.

Weiss law with the parameters $\chi(0)=8\times10^{-5}$ emu/mole Yb, $\theta_p=-48$ K, and $\mu_{\rm eff}=3.90\mu_B$ per Yb atom (calculated on the basis of five Yb atoms per formula unit). This value is somewhat higher than that obtained in Ref. 5 ($3.46\mu_B$), but still much lower than the free-ion value $4.54\mu_B$. The impurity content of our sample is also too small to account for such a large deviation. With the assumption of the $6g$ site being occupied by $Yb^{3+}$ ions and the $4d$ site by $Yb^{2+}$, made in Ref. 5, one obtains $\mu_{\rm eff}\simeq5.1\mu_B$ for the Yb ions at the $6d$ site, which is too high for assignment to a $Yb^{3+}$ ion. This observation leads to the conclusion that the Yb ions located at the $4d$ sites significantly contribute to the paramagnetic susceptibility of $Yb_5Si_3$, and thus that they cannot be in the diamagnetic $Yb^{2+}$ charge state. In the following analysis, we assume that the $6g$ sites are occupied by stable $Yb^{3+}$ ions, but that the weakly paramagnetic Yb ions at the $4d$ sites exhibit an intermediate valence (IV) state.

An approach describing the behavior of IV systems is the interconfiguration fluctuation model developed by Sales and Wohlleben.[11] This model assumes that the $Yb^{2+}$ and $Yb^{3+}$ configurations are almost degenerate, with the $Yb^{2+}$ configuration as the ground state. The magnetic susceptibility of a Yb ion in the IV state may be expressed as

$$\chi^{\rm IV}(T)=\frac{\mu_{\rm eff}^2[1-\vartheta(T)]}{3k_B(T+T_{\rm sf})}, \tag{2}$$

where $\mu_{\rm eff}=4.54\mu_B$ is the effective magnetic moment associated with the $4f^{13}$ excited state, $T_{\rm sf}$ stands for the spin fluctuation temperature describing fluctuations between both configurations, and $\vartheta(T)$ is the mean occupation of the ground configuration (the fractional valence) and is given by

$$\vartheta(T)=\frac{1}{1+8\exp[-E_{\rm ex}/(T+T_{\rm sf})]}. \tag{3}$$

In the latter equation $E_{\rm ex}$ is the energy difference between the $4f^{13}$ and $4f^{14}$ configurations. With our hypothesis of the $6g$ sites occupied by $Yb^{3+}$ ions and the $4d$ sites by IV Yb ions, the total magnetic susceptibility of $Yb_5Si_3$ can be represented as

$$\chi(T)=0.4\chi^{\rm IV}(T)+0.6\chi^{\rm Yb^{3+}}(T), \tag{4}$$

where $\chi^{\rm Yb^{3+}}$ is the magnetic susceptibility of a stable $Yb^{3+}$ ion, given (at temperatures high enough to neglect crystal field effects) by the Curie-Weiss (CW) law

$$\chi^{\rm Yb^{3+}}(T)=\frac{\mu_{\rm eff}^2}{3k_B(T-\theta_{\rm CW})}, \tag{5}$$

with $\mu_{\rm eff}=4.54\mu_B$. The solid line in Fig. 6 is a least-square fit to Eq. 4, for T>200 K, of the experimental $\chi^{-1}(T)$ variation in $Yb_5Si_3$. The fitting parameters are as follows: $T_{\rm sf}=1300$ K, $\theta_{\rm CW}=-10$ K, and $E_{\rm ex}$ varying between 10 and 300 K. The effective valence of the Yb ions at the $4d$ sites, estimated from Eq. (3), is found to be 2.89 at 800 K, and to hardly change with temperature. The independence of the Yb effective valence on temperature is here a direct consequence of the very small energy difference $E_{\rm ex}$ between the two Yb configurations—in the temperature range of our measurements both states are already strongly thermally populated. This value is in good agreement with the mean valence of 2.88 obtained from the $L_{\rm III}$-edge x-ray measurements. The large value of $T_{\rm sf}$ results in a strong reduction of the paramagnetic susceptibility of the Yb ions located at the $4d$ sites with respect to the susceptibility expected for a free $Yb^{3+}$ ion. Such a behavior is often found in intermetallic ytterbium compounds where the hybridization of the $4f$ electronic states with the conduction electron is rather strong,[12] resulting in a Yb valence somewhat lower than 3. In turn, the magnitude of the $\theta_{\rm CW}$ value derived here for the $6g$ Yb ions is typical of compounds with stable or weakly hybridized $Yb^{3+}$ ions. Moreover, a remarkable deviation of the experimental $\chi^{-1}(T)$ dependence from the model curve observed at low temperatures (see Fig. 6) results from crystal-field effects. This hypothesis of an almost trivalent strongly hybridized Yb ion at the $4d$ site will be shown to account well for the experimental data in $Yb_5Si_3$ (see Sec. VII B).

## VII. DISCUSSION

It was previously suggested[5] that $Yb_5Si_3$ is a heterogeneous mixed-valence system with 60% of Yb ions in the 3+ and 40% in the 2+ charge state. Indeed, the hyperfine interaction experiments show two components in the zero-field Mössbauer and PAC spectra with the intensity ratio 3:2. However, the suggestion about the $Yb^{2+}$ state cannot be maintained: the temperature dependence of the EFG (see Fig. 3) exhibits a strong thermal variation for the two Yb sites. Such a dependence can be understood only when the $4f$ electron shell is not completely filled. Then, from the zero-field hyperfine interaction experiments, a $Yb^{2+}$ charge state can be obviously excluded for Yb ions in both sublattices of $Yb_5Si_3$.

### A. Crystal electric-field effects

In view of the results obtained with these three microscopic techniques, the $4f$ electron shell of the Yb ion seems to be in an almost trivalent charge state for both the $6g$ and $4d$ sites. On the other hand, the magnetic-susceptibility measurements show a Yb effective magnetic moment smaller than that expected for the free $Yb^{3+}$ ion. It is well known that the CEF interaction can lead to a moment reduction, at least at low temperature when all the CEF states are not equally populated. The magnitude of the CEF interaction can be estimated in $Yb_5Si_3$ from the EFG temperature dependence, since the measurements were performed in an unusually wide temperature range. A quantitative description of the EFG temperature dependence involves the CEF formalism.[13] Since the Yb atoms occupy lattice sites with a rather low symmetry, the number of independent CEF parameters is high: nine for the $6g$ sites and six for the $4d$ sites.[13] It is therefore not possible to fit unambiguously all these parameters from the EFG thermal variation. Several attempts have been performed with a limited number of the CEF parameters. These simulations lead us to two conclusions: (1) the first excited CEF level must be around 180 K for the $4d$ site, and around 200 K for the $6g$ site; and (2) the overall level splitting is between 1000 and 1500 K for all Yb ions. Such a value is unusually large for intermetallic Yb compounds, where it usually amounts to a few 100 K.

The large value of the CEF splitting cannot explain the low effective magnetic moment value: using model CEF parameters that approximately reproduce the EFG thermal variation, the calculated thermal variation of $1/\chi$ is found to be practically linear above 200 K with a slope characteristic of the free $Yb^{3+}$ ion. The inset of Fig. 6 shows the low-temperature part of $1/\chi$ in $Yb_5Si_3$; the observed curvature is roughly consistent with the derived CEF level scheme.

### B. Hybridization effects and model for $Yb_5Si_3$

Hybridization of the $4f$ electrons and the band electrons in Ce- or Yb-based alloys is a rather common feature.[12] It leads to such properties as the Kondo effect, the intermediate valence of the rare-earth ion, and the ''heavy electron'' behavior. In these compounds, the magnetic susceptibility shows a paramagnetic behavior and often follows a Curie-Weiss behavior with a large negative paramagnetic Curie temperature ($\sim -100$ K); the Yb or Ce sublattice usually shows no magnetic ordering down to 0 K. Some examples of almost trivalent Yb alloys are known, where hybridization is rather strong:[14] cubic $YbAl_3$, hexagonal YbCuAl, or tetragonal $YbPd_2Si_2$ and $YbCu_2Si_2$. In YbCuAl and $YbPd_2Si_2$ the presence of CEF levels, although broadened by the hybridization, is well documented by inelastic neutron scattering;[15–17] in these latter compounds and in $YbCu_2Si_2$, a sizable thermal variation of the electric-field gradient at the Yb site has been observed by Mössbauer spectroscopy.[18–20] In order to account for all the properties measured in $Yb_5Si_3$, here we propose the following model: the Yb ions on the two sites both have a valence close to 3, in agreement with the zero-field hyperfine measurements and the $L_{III}$-edge x-ray-absorption results, but the hybridization strength is different on the two sites.

The Yb ion at the $6g$ site (60% component) is in a trivalent valence state, with probably a weak $4f$-conduction electron hybridization responsible for the absence of magnetic ordering down to 0.03 K. By contrast, the Yb ion at the $4d$ site (40% component) is strongly hybridized. This picture is in agreement with the Mössbauer spectrum with applied magnetic field and with the magnetic susceptibility data. The magnetic-susceptibility of the $4d$ Yb ion is well described by the interconfiguration fluctuation model with a large spin fluctuation temperature $T_{sf} \simeq 1300$ K. The electric-field gradient at the $4d$ site shows a sizable thermal variation because the overall CEF splitting is somewhat greater or of the same magnitude as $T_{sf}$, as estimated in Sec. VII A.

The alloy $Yb_5Si_3$ can then be classified as a ''heterogeneous hybridization'' Yb compound and, to our knowledge, it is the first unambiguous example of this type. One can speculate that the existence of two crystallographically inequivalent sites can favorize the appearance of different hybridization strengths on each site. In this respect, the situation in $Yb_5Si_3$ is different from that in known heterogeneous mixed-valence Yb alloys like YbPd (Ref. 21) or $Yb_4As_3$,[22,23,6] where a phase transition occurs from a high-temperature phase with a unique Yb site to a low-temperature charge-ordered phase with (in principle) two inequivalent Yb sites. In $Yb_5Si_3$, no phase transition is detected in the thermal variation of the resistivity up to 600 K,[5] or of the magnetic susceptibility up to 800 K.

## VIII. CONCLUSION

We reexamined the properties of the Yb alloy $Yb_5Si_3$, which was previously thought to be a heterogeneous mixed-valence system, with $Yb^{3+}$ ions occupying the 60% $6g$ site and $Yb^{2+}$ ions occupying the 40% $4d$ site of the $Mn_5Si_3$-type hexagonal structure. We carried out zero-field and in-field $^{170}$Yb Mössbauer absorption spectroscopy, perturbed angular correlations of $\gamma$ radiation on $^{172}$Yb, x-ray absorption near the Yb $L_{III}$ edge, and magnetic-susceptibility measurements in an extended temperature range in $Yb_5Si_3$. We found that while the zero-field Mössbauer, the PAC, and $L_{III}$-edge data point to a valence close to 3 for the Yb ions on both sites, the in-field Mössbauer and magnetic measurements indicate that the Yb ions at the $4d$ site have a paramagnetic susceptibility much smaller than expected for a free $Yb^{3+}$ ion. We propose a model to interpret these findings, in the frame of the $4f$ conduction-electron hybridization often occurring in intermetallic Yb compounds: the hybridization strength is different for the Yb ions at the two sites, being large for the Yb ions at the $4d$ site and much weaker for the Yb ions at the $6d$ site. We also found that the crystal-field interaction leads to an unusually large splitting of the Yb levels, of the order of 1000–1500 K. $Yb_5Si_3$ therefore is not a classical heterogeneous mixed-valence system, but rather the first clear example of a Yb compound where the two crystallographic sites are occupied by almost trivalent Yb ions with different hybridization strengths.

## ACKNOWLEDGMENTS

Research support was received under the France-Poland Scientific Project and KBN Grant No. PB 523/P3/93/05.

[1] I. Abbati, L. Braicovich, C. Carbone, J. Nogami, I. Lindau, I. Iandelli, G. Olcese, and A. Palenzona, Solid State Commun. **62**, 35 (1987).
[2] P. Bonville (unpublished).
[3] C. Engkagul, R. Selim, T. Mihalisin, and P. Schlottmann, Phys. Rev. B **35**, 3686 (1987).
[4] P. Bonville, F. Gonzalez-Jimenez, P. Imbert, D. Jaccard, G. Jéhanno, and J. Sierro, J. Phys. Condens. Matter **1**, 8567 (1989).
[5] F. Canepa, S. Cirafici, F. Merlo, and A. Palenzona, J. Magn. Magn. Mater. **118**, 182 (1993).
[6] K. Królas, M. Rams, P. Bonville, F. Canepa, and A. Ochiai, Physica B **230,** 263 (1997).
[7] E. Bauer, Le Tuan, R. Hauser, E. Gratz, F. Holubar, G. Hilscher, W. Perthold, C. Godart, E. Alleno, and K. Hiebl, Phys. Rev. B **52**, 4327 (1995).
[8] K.-G. Plingen, B. Wolbeck, and F.-J. Schreder, Nucl. Phys. A **165**, 97 (1971).
[9] K. Królas and M. Rams, Hyperfine Interact. **1**, 159 (1996).
[10] P. Bonville, P. Imbert, G. Jéhanno, and F. Gonzalez-Jimenez, J. Phys. Chem. Solids **39**, 1273 (1978).
[11] B. C. Sales and D. K. Wohlleben, Phys. Rev. B **35**, 1240 (1975).
[12] N. B. Brandt and V. V. Moshchalkov, Adv. Phys. **33**, 372 (1984).
[13] A. Abragam and B. Bleaney, *Electron Paramagnetic Resonance of Transition Ions* (Clarendon, Oxford, 1970).
[14] Z. Fisk and M. B. Maple, J. Alloys Compd. **183**, 303 (1992).
[15] A. P. Murani, W. C. M. Mattens, F. R. de Boer, and G. H. Lander, Phys. Rev. B **3**, 52 (1985).
[16] W. Weber, E. Holland-Moritz, and A. P. Murani, Z. Phys. B **76**, 229 (1989).
[17] G. Polatsek and P. Bonville, Z. Phys. B **88**, 189 (1992).
[18] P. Bonville and J. A. Hodges, J. Magn. Magn. Mater. **47**, 152 (1985).
[19] P. Bonville, J. Hammann, J. A. Hodges, P. Imbert, G. Jéhanno, M. J. Besnus, and A. Meyer, Z. Phys. B **82**, 267 (1991).
[20] K. Tomala, D. Weschenfelder, G. Czjzek, and E. Holland-Moritz, J. Magn. Magn. Mater. **89**, 143 (1990).
[21] P. Bonville, J. Hammann, J. A. Hodges, P. Imbert, and G. Jéhanno, Phys. Rev. Lett. **57**, 2733 (1986).
[22] A. Ochiai, T. Suzuki, and T. Kasuya, J. Phys. Soc. Jpn. **59**, 4129 (1990).
[23] P. Bonville, A. Ochiai, T. Suzuki, and E. Vincent, J. Phys. (France) I **4**, 595 (1994).